The Cloud Aerosol Interaction and Precipitation Enhancement Experiment (CAIPEEX): overview and preliminary results

J. R. Kulkarni*, R. S. Maheskumar, S. B. Morwal, B. Padma Kumari, M. Konwar, C. G. Deshpande, R. R. Joshi, R. V. Bhalwankar, G. Pandithurai, P. D. Safai, S. G. Narkhedkar, K. K. Dani, A. Nath, Sathy Nair, V. V. Sapre, P. V. Puranik, S. S. Kandalgaonkar, V. R. Mujumdar, R. M. Khaladkar, R. Vijayakumar, T. V. Prabha and B. N. Goswami

Indian Institute of Tropical Meteorology, Dr Homi Bhabha Road, Pashan, Pune 411 008, India

While the demand for enhancing rainfall through cloud seeding is strong and persistent in the country, considerable uncertainty exists on the success of such an endeavour at a given location. To understand the pathways of aerosol–cloud interaction through which this might be achieved, a national experiment named Cloud Aerosol Interaction and Precipitation Enhancement EXperiment (CAIPEEX) in two phases, was carried out. The rationale of CAIPEEX, the strategy for conducting the experiment, data quality and potential for path-breaking science are described in this article. Pending completion of quality control and calibration of the CAIPEEX phase-II data, here we present some initial results of CAIPEEX phase-I aimed at documenting the prevailing microphysical characteristics of aerosols and clouds and associated environmental conditions over different regions of the country and under different monsoon conditions with the help of an instrumented research aircraft. First-time simultaneous observations of aerosol, cloud condensation nuclei (CCN) and cloud droplet number concentration (CDNC) over the Ganges Valley during monsoon season show very high concentrations (> 1000 cm^{-3}) of CCN at elevated layers. Observations of elevated layers with high aerosol concentration over the Gangetic valley extending up to 6 km and relatively less aerosol concentration in the boundary layer are also documented. We also present evidence of strong cloud–aerosol interaction in the moist environments with an increase in the cloud droplet effective radius. Our observations also show that pollution increases CDNC and the warm rain depth, and delays its initiation. The critical effective radius for warm rain initiation is found to be between 10 and 12 μm in the polluted clouds and it is between 12 and 14 μm in cleaner monsoon clouds.

Keywords: Aircraft observation, CAIPEEX, cloud seeding, cloud–aerosol interaction, cloud condensation nuclei.

INDIAN agriculture being largely (two-thirds of the cropped area) rainfed, any drought-like condition leads to major loss of agricultural productivity and seriously affects livelihood of a large population[1]. While major droughts affect the whole country, even during a 'normal' monsoon year there are regions within the country that may experience drought-like conditions[2]. Therefore, there is considerable demand on increasing rainfall in these regions by whatever possible means. Cloud seeding by appropriate aerosols has been considered by many as the panacea for the problem[3]. Unfortunately, jury has been divided on the effectiveness of seeding on enhancing rainfall[4,5]. Early observations from aircraft records and meteorological observations over India indicated predominance of warm clouds[6] and warm-cloud seeding received much attention[7]. The Indian Institute of Tropical Meteorology (IITM) carried out cloud seeding experiment over Baramati region, Maharashtra, during the period 1973–74, 1976 and 1979–1986 using salt as the hygroscopic seeding material[8–11]. The results indicated an approximate increase of 24% in the rainfall[11]. However, this increase was with a caveat that it occurred when area seeding rather than isolated cloud seeding was conducted. The earlier experiment identified the conditions necessary for cloud seeding, but the experiment ended before the technique was verified on independent samples. Since then, new techniques for cloud seeding, such as flares have been introduced. Hence it became necessary to revisit the problem of cloud seeding scientifically, with emphasis on the role of aerosol–cloud interactions on it.

With advances in seeding technology as well as the recent accessibility with the state-of-the-art instrumentation for cloud microphysical measurements, several international experiments have been carried out in the recent

*For correspondence. (e-mail: jrksup@tropmet.res.in)

years. These experiments examined possible enhancement of precipitation through cloud seeding[5]. There was however, considerable uncertainty over the outcome of these experiments leading to either increase, decrease or no change in precipitation. Therefore, it is not scientifically sound to carry out operational cloud seeding at a particular location without establishing the feasibility of precipitation enhancement at that location.

Rather disparate results of different experiments and the resultant uncertainty in the effectiveness of cloud seeding are linked to the basic principle on which these experiments are based. At the heart of the issue are the cloud condensation nuclei (CCN), which are aerosol particles on which water vapour condenses and initial cloud droplets form and grow through the collision–coalescence process to bigger droplets and eventual precipitation[12]. The collision–coalescence becomes more efficient with larger effective radius of the cloud droplets. Addition of giant CCN (GCCN having 5–10 μm radius; for example, sea salt) to a cloud with numerous small droplets can accelerate the rain-formation process[13,14]. Thus, most cloud seeding efforts aim at putting certain amount of specific types of aerosol with the potential for conversion to large CCN in favourable regions of the cloud for accelerated growth. The size distribution of the CCN is, therefore, crucial for effectiveness of the rain formation. For example, if the CCN distribution is skewed towards small size (< 1 μm), it would produce numerous small droplets, which may significantly reduce the effectiveness of the collision–coalescence process and delay the warm rain formation[15–20]. Therefore, effectiveness of seeding in modifying the cloud and enhancing precipitation depends crucially on the background CCN distribution (type and concentration of aerosols). If the background CCN distribution is such that enough concentration of larger size is available, any addition of such CCN is unlikely to enhance precipitation[5].

In order to understand interaction between the aerosols and the clouds, it is essential to make simultaneous observations of aerosols, CCN and cloud droplet number concentration (CDNC) as a function of depth of the cloud. Also, in order to select a site for the cloud seeding experiments, it is necessary to have a clear idea of the background CCN distribution, and macrophysical and microphysical characteristics of clouds over climatically divergent regions of the country. Unfortunately, such observations did not exist, especially during the monsoon season. Several important experiments have been carried out in the recent years over the Indian region such as the Indian Ocean Experiment (INDOEX)[21–23], Indian Space Research Organisation (ISRO)-conducted Aerosol Radiative Forcing over India (ARFI) and Integrated Campaign for Aerosols, gases and Radiation Budget (ICARB)[23,24]. These experiments primarily aim at documenting variability and direct radiative effects of aerosols. These and a few other experiments were conducted mainly during pre-monsoon or winter seasons. Cloud Aerosol Interaction and Precipitation Enhancement EXperiment (CAIPEEX) aims at filling some gaps in our knowledge on cloud–aerosol interaction and cloud microphysics in different regions of India, and response of cloud microphysics to the seeding for rain enhancement. In order to estimate the potential for local precipitation enhancement through cloud seeding, a good knowledge of climatology of aerosols and CCN together with the prevailing cloud characteristics, and dynamic and thermodynamic properties of the atmosphere are essential. As the aerosol loading and their characteristics are changing (increasing) rapidly due to anthropogenic activity, such data collected a few decades ago (such as the IITM experiments during the seventies and early eighties) are not useful for making an estimate of the current potential for cloud seeding. Also, since simultaneous observations of aerosols, CCN and cloud microphysical parameters during recent years over India are not currently available, there is a great need for an experiment to make these measurements over India. This is the genesis of the CAIPEEX. Detailed science plan and associated details of CAIPEEX are provided online at http://www.tropmet.res.in/~caipeex/

Objectives and outline of CAIPEEX

With the above background, the CAIPEEX is planned to achieve the following two major objectives:

(i) To make necessary simultaneous measurements of microphysics of aerosols, CCN, cloud parameters (number concentration, liquid water, particle size, etc.) and large-scale meteorological conditions to document and understand the pathways through which aerosols interact with clouds and influence precipitation over the continental Indian monsoon region.

(ii) To quantify the efficacy of seeding in precipitation enhancement over a suitable location in India. A related objective is also to test the efficiency of different seeding materials in this process. (Also to formulate guidelines for cloud seeding based on direct observations.)

To achieve these objectives, the experiment was planned to be carried out in two phases. Due to diverse climatic conditions across the country and large seasonal cycle, phase-I of CAIPEEX was conducted during May–September 2009 from six base locations, namely Pune, Pathankot, Hyderabad, Bareily, Bengaluru and Guwahati, representing different environmental conditions ranging from semi-arid Pathankot, Pune and Hyderabad, to moist monsoon conditions over Bengaluru, Bareily and Guwahati, aimed at collecting simultaneous microphysical properties of aerosols, CCN and clouds. One instrumented aircraft was used for the purpose. For collecting back-

ground thermodynamic data, radiosonde ascents were also conducted in conjunction with aircraft-measured parameters.

Phase-II of CAIPEEX was planned to focus on the second objective, namely to quantify the efficacy of seeding in precipitation enhancement and to understand the mechanism of aerosol–cloud dynamics interaction responsible for the process. For this purpose together with the seeding experiments, growth and decay of the clouds and their microphysical characteristics need to be measured. Based on preliminary results from phase-I, Hyderabad was considered as the base station for phase-II experiment. Hyderabad is located in the rainshadow region during the southwest monsoon on the eastern side of the Western Ghats mountains, and the region around it is vulnerable to drought conditions. In order to be able to delineate the contribution of seeding from naturally occurring precipitation, sample size needs to be sufficiently large. As a result, the phase-II experiment was between the monsoon and post-monsoon seasons of 2010 and 2011. A double-blind randomized procedure in the seeding experiments was followed to have statistical confidence in the results.

The first year operations of phase-II were carried out during September and October 2010. Two instrumented aircraft, one for solely seeding (called seeder aircraft) and the other for both seeding and cloud microphysics measurements (called cloud physics aircraft) were used. For monitoring the clouds, a C-band radar was installed at Solapur, about 267 km away from Hyderabad. During the phase-II second year, this radar was located in Mahabubnagar, approximately 100 km away from the Hyderabad base. In addition, a S-band radar of India Meteorological Department (IMD) located at Hyderabad was also used. The main objectives of CAIPEEX phase-II first year were: (i) to carry out a pilot phase of main cloud seeding experiment and (ii) continuation of the study of cloud microphysics and cloud–aerosol interaction over land and oceanic regions undertaken in phase-I.

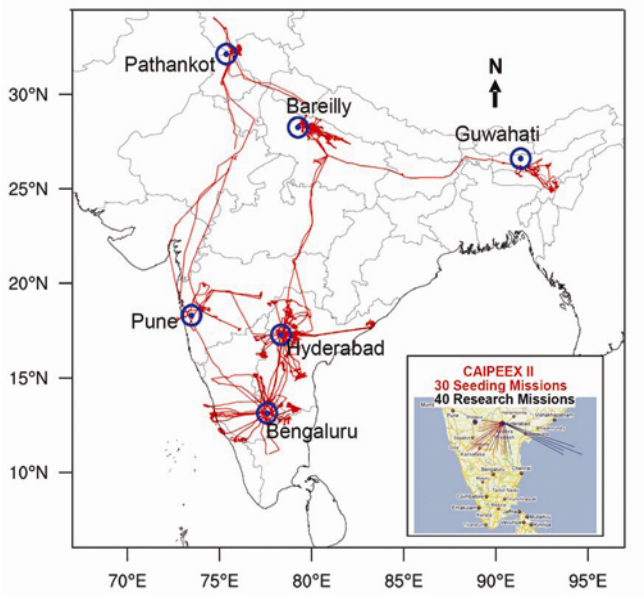

Figure 1. IOP bases from which flights were coordinated, and some typical flight paths during CAIPEEX phase-I. (Inset) CAIPEEX phase-II flights.

The first objective was attempted in two ways: (i) using research and seeder aircraft and (ii) using seeder, research aircraft and a radar. The first method involves measurements of the cloud microphysical parameters by the research aircraft before and after seeding to test the physical hypothesis of the seeding. The second method rests on examining the evolution of the cloud structure after seeding by radar observations, in addition to research aircraft measurements. Efforts were directed to: (i) test these two options, (ii) establish coordination among all three components and (iii) test technical feasibility of highly intense avionics-centred activity. About 200 h of flying was completed by both aircraft. The research aircraft was flown for 120 h and the seeder aircraft for 80 h. Figure 1 (inset) shows the flight tracks of the aircraft during phase-II first year.

The second year operations of CAIPEEX phase-II were conducted from September to November 2011. An instrumented research and a seeder aircraft carried out the research as well as seeding experiments. Both the aircraft were flying together for 250 h. A fully randomized cloud seeding experiment was conducted using both hygroscopic flares and salt powder as seeding agents. C-band Doppler radar and S-band Doppler radar of IMD were used during the campaign. The randomized cloud seeding requires that the studied cloud is in the field-of-view of the radar. A CAIPEEX convective forecast algorithm developed at IITM and mesoscale forecasts from the National Centre for Medium Range Weather Forecasting (NCMRWF), both at 3 km resolution have been routinely used for randomized cloud seeding decisions. Research flights to study aerosol distribution and cloud microphysics over peninsular India, coastal convection and sampling of convective clouds at the periphery of deep convection were also carried out. Apart from the airborne operations, a full-fledged Integrated Ground Observational Campaign (IGOC) at the central location, Mahabubnagar, of aircraft operations was also carried out. Surface-based instruments to measure boundary-layer parameters, aerosols, CCN, trace gases, state parameters and atmospheric thermodynamics were deployed at the IGOC site. TIFR Balloon facility, Space Physics Laboratory (SPL) and University of Pune (UoP) participated in the IGOC.

As the data collected during these campaigns involving aircraft instruments require careful quality control, the phase-II data are not yet ready for scientific analysis. Therefore, we will not present results from the CAIPEEX phase-II in this article. We describe CAIPEEX phase-I in

some detail here and present a glimpse of the results that can be derived from it.

Details of CAIPEEX phase-I

Bases and dates of observations

Phase-I was conducted during the period 14 May–30 September 2009. The aerosol (and hence CCN) distributions vary significantly from pre-monsoon to monsoon and post-monsoon season, and there is considerable variability of dynamic and thermodynamic conditions across the country during this period. Considering the logistic factors, six base stations were selected. Figure 1 shows the bases from where the flights were operated and respective flight tracks during phase-I. Table 1 shows the dates and flying hours from these bases. The inset in Figure 1 corresponds to the flight tracks for both research and seeded missions during CAIPEEX phase-II first year. A total of 219 h of flying was done during the period. The aircraft and the instruments used are described below.

Aircraft

A Piper Cheyenne model PA-31 T instrumented aircraft was utilized in the programme. The aircraft was certified for flying into known icing conditions and had a pressurized cabin. It had capacity to carry a scientific crew of four persons, and climb up to a maximum altitude of 8.5 km, with a range of 1200 nautical miles, and endurance of 5 h with scientific payload. The minimum rate of climb was 60.96 m/min.

List of instruments

The aircraft was fitted with several instruments for measuring atmospheric state parameters (air temperature, pressure, humidity, etc.) and Global Positioning System position. The list of instruments, their range, accuracy, resolution and frequency and measured parameters are given in Tables 2–4. In addition, measurements of ice nuclei, black carbon and trace gases were also carried out. The filters for collecting the ice nuclei were provided by the Department of Atmospheric and Space Sciences (DASS), University of Pune. The measurements were taken for 3 min, mostly in the cloud base. Few filters were also taken at higher altitude, whenever it was considered to be necessary. The samples are analysed in the cloud chamber available at DASS. The black carbon measurements were done using an aethalometer from IITM. The trace gas instruments did not work satisfactorily during the first-year campaign. Simultaneous with the aircraft flights, the radiosonde flights were operated from the respective bases.

The Aircraft Integrated Meteorological Measurement System (AIMMS) measures the weather parameters, namely barometric pressure, temperature, humidity and three components of wind. It also measures the aircraft position and other parameters like pitch and roll. For the winds, the Kalman Filter Digital Signal Processing technique is used. AIMMS consists of four components; an Air Data Probe (ADP), a carrier-phase geostationary positioning satellite (GPS) measurement module, an inertial measurement unit (IMU) and the Central Processing Module (CPM). The ADP is mounted below the lower wing surface, whereas the other three modules are located in the cockpit. The system gives position and velocity information from the GPS with six axis inertial rates from three rate gyros and accelerometers of IMU, and aerodynamically corrected 3D aircraft-relative flow vector data from ADP. The CPM combines data from ADP and GPS to determine winds to the accuracy of 0.5 ms^{-1}. It requires power supply of 28 VDC, 100 mA for the system and 28 VDC, 8 A for the anti-ice system.

Selection of clouds and profiling strategy

Based on the analysis of synoptic situation and prediction of thermodynamic conditions, a working area was chosen with high potential for the development of cumulus (Cu) clouds. It would be preferable to look for an isolated Cu cloud in its growing stage at the up-shear part of a cloud cluster with deep convective elements (so that we will have a succession of growing towers until we reach the maximum cloud top). But a field of clouds at different heights is also a good choice. In some situations, deep convective clouds were also profiled from top to bottom. This provided one of the rare and first time continental datasets of cloud microphysics with cloud profiling up to a height of 7–7.5 km above the surface.

To understand the aerosol effects on the clouds, it is important to make vertical profiles of the cloud

Table 1. Location of the bases, observation period and flying hours for CAIPEEX phase-I. In addition to these flight records, there were transition flights connecting different Intensive Observation Period locations

IOP location	Observation period	Flying hours
Pune	17–21 May	4.25
Pathankot	23–29 May	16.45
Bengaluru	1–8 June	7.55
Hyderabad	11–23 June	12.15
Bengaluru	26 June–13 July	9.55
Bareilly	15–24 July	17.15
Hyderabad	14–18 August	9.10
Bareilly	19–26 August	10.50
Guwahati	29 August–15 September	13.15
Pune	16–25 September	20.25
Hyderabad	27–29 September	12.30

Table 2. Details of aircraft instruments: State parameters and avionics

Variable	Make/instrument	Range	Accuracy	Resolution	Frequency
Air temperature	Rosemount 102DB1CB	–50°C to +50°C	0.1°C	0.01°C	1 Hz
Air temperature (reverse flow)	0.038″ Dia Bead Thermistor	–30°C to +50°C	0.05°/0.3°C	0.01°C	< 1 s TC
Relative humidity (reverse flow)	Thermoset polymer RH Sensor	0% to 100% RH	2% RH	0.1% RH	5 s TC @ 20°C
Barometric pressure	MEMS Pressure Sensor	0 to 110,000 Pa	100 Pa	10 Pa	20 Hz
Wind (all the three components)	Extended Kalman Filter (EKF)		0.50 m/s @ 75 m/s TAS	0.01 m/s	5 Hz
Position (lat./long.)	WAAS DGPS		2 m	< 1 m	5 Hz
Altitude	WAAS DGPS	–300 to 18,000 m	5 m	< 1 m	5 Hz
Geometric altitude	King KRA 405 Radar Altimeter	0 to 2000 ft	3% < 500 ft 5% > 500 ft	0.48 ft (0.15 m)	
Aircraft attitude (roll, pitch and yaw; °)	MEMS IMU/GPS/EKF	–60° to +60°	0.1°	0.01°	5 Hz
Angle of attack and side-slip (°)	MEMS Pressure Sensor	–15° to +15°	0.03° @ 150 m/s	0.001° @ 150 m/s	20 Hz
True air speed	MEMS Pressure Sensor	0 to 150 m/s	0.1 m/s	0.01 m/s	20 Hz
Logging, telemetry and event markers	ESD DTS (GPS)				1 Hz
Black carbon aerosols	Aethalometer (AE–42)		5 ng/m^3		1 min

Table 3. Aerosol and cloud microphysics instruments from Droplet Measurement Technologies Inc. (DMT) such as cloud droplet probe (CDP), cloud imaging probe (CIP), passive cavity aerosol spectrometer probe (PCASP), cloud condensation nuclei (CCN) counter, their range, resolution and sampling frequency, and variables measured by each instrument

Variable	Make/instrument	Range	Resolution	Frequency
Cloud droplet spectra	DMT CDP	2 to 50 μm	1 to 2 μm, 30 bins	1 Hz
Cloud particle spectra	DMT CIP	25 to 1550 μm	25 μm, 62 bins	1 Hz
Cloud particle image	DMT CIP	25 to 1550 μm	25 μm	
Liquid water content	DMT LWC-100	0 to 3 g/m^3	0.01 g/m^3	1 Hz
Liquid water content	CDP calculated	> 3 g/m^3		1 Hz
Isokinetic aerosol inlet	Brechtel double-diffuser inlet	28 lpm		100 m/s
Aerosol spectrometer	DMT PCASP SPP-200	0.1 to 3 μm	0.02 μm, 30 bins	1 Hz
CCN	DMT CCN counter	0.5 to 10 μm 0.1 to 1.2% SS	0.5 μm, 20 bins	1 Hz

Table 4. Trace gases

Measurement	Range
O_3	1 ppb–100 ppm
SO_2	0.3–200 ppb
CO	< 5 ppb
CO_2	
$NO/NO_2/NO_y$	NO ~ 10 ppt @ 10 s NO_2 ~ 50 ppt @10 s NO_y ~ 100 ppt @10 s

microphysical properties (CDNC, liquid water and effective radius) from the cloud base to the height where all the cloud water is exhausted. This is the most straightforward way to document the evolution of the clouds and the precipitation formation processes in them. This way we can follow the cloud top as it develops, and are less prone to precipitation falling from above from an unknown altitude. Every cloud penetration is at least for 5 s or longer and preferably on a level flight, so that regions near the convective cores of the clouds could also be sampled.

Data and quality control

The scientific instruments utilized in the programme were factory calibrated at Droplet Measurement Technologies Inc. (DMT). For liquid water content (LWC), the cloud droplet measurements by hot-wire liquid water probe (HW-LWC) are considered to be more reliable. Baseline corrections for HW-LWC were done by taking into consideration the reading of the previous 100 s. The LWC

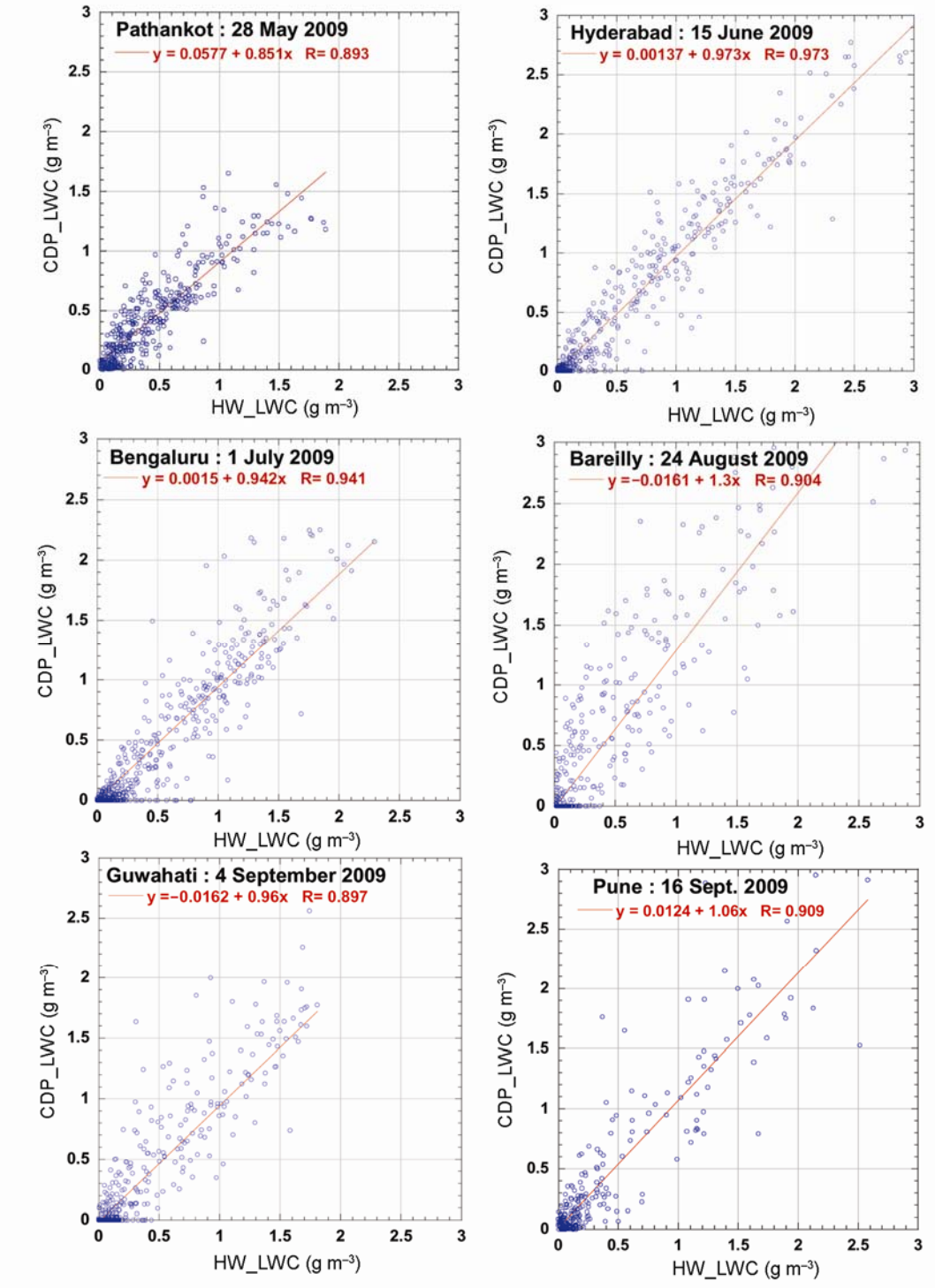

Figure 2. Comparison of LWC measured from Johnson Williams hot-wire probe (HW_LWC) and derived from cloud droplet probe (CDP_LWC) over six IOP bases.

measured by Cloud Droplet Probe (CDP) was compared with HW-LWC from time to time for assessment on the performance of CDP. A few days of comparison between CDP LWC and HW-LWC is provided in Figure 2. A correlation of 0.85 or greater is noted in the cases presented. The cloud droplet probe was size calibrated from time to time in the field from known size of beads. The Cloud Imaging Probe (CIP) data were post-processed (with the codes provided by the manufacturer) to reduce the artefacts due to shattering effect of large hydrometeors by taking into account of the inter-arrival time ($\approx 10^{-6}$ s) of individual droplets[25]. The Passive Cavity Aerosol

Spectrometer Probe (PCASP), the CCN counter and the CIP probe were factory-calibrated. These instruments performed satisfactorily during the experiment period. For accurate CCN concentrations, pressure correction was applied by a fraction of ambient pressure to the CCN counter pressure of ≈ 500 hPa. The actual supersaturation (SS) drops by about 0.07% SS per 100 hPa decrease in the CCN counter; effective SS was calculated for the entire flight. The meteorological parameters such as temperature, relative humidity, pressure and wind direction were compared with *in situ* radiosonde observations.

Results from CAIPEEX phase-I

Simultaneous observations of particle size distributions of aerosols, CCN and cloud droplets (cloud microphysics parameters, aerosols and CCN) over different parts of the country from May to September 2009 represent an unprecedented dataset for studying various aspects of aerosol–cloud interactions over the region. The observations during phase-I were made from pre-monsoon to active monsoon conditions and also in the break periods during monsoon. An overview of the number concentration of aerosols (N_a), CDNC and CCN concentration. (N_{CCN}; CCN concentrations were typically measured with a SS of 0.2%, 0.4% and 0.6%. CCN with a constant SS of 0.4 was used in the analysis presented in this study.) All data of CCN and aerosol number concentration were cloud-screened with a condition of CDNC < 20 cm^{-3}. The area averaged rainfall (Tropical Rainfall Measuring Mission (TRMM)) for each 1° × 1° box over the base locations (listed in Table 1) where we have simultaneous observations of aerosol, CCN and CDNC (N_a, N_{CCN} and CDNC) is presented in Figure 3. It is interesting to note that N_a and N_{CCN} did not decrease drastically after the rain events. This indicated that aerosols did not get removed by scavenging and there is a constant source of aerosols/CCN throughout the monsoon season. CCN concentrations are higher than aerosol concentrations at most locations due to the fact that measurement of aerosol concentration by PCASP is limited to only accumulation-mode particles. Average CDNC is in the 200–500 cm^{-3} range. To study the high aerosol concentrations and their persistence over the whole CAIPEEX campaign, vertical profiles of cloud-screened aerosol number concentration and CCN number concentration are analysed in the next section along with the air-mass trajectories.

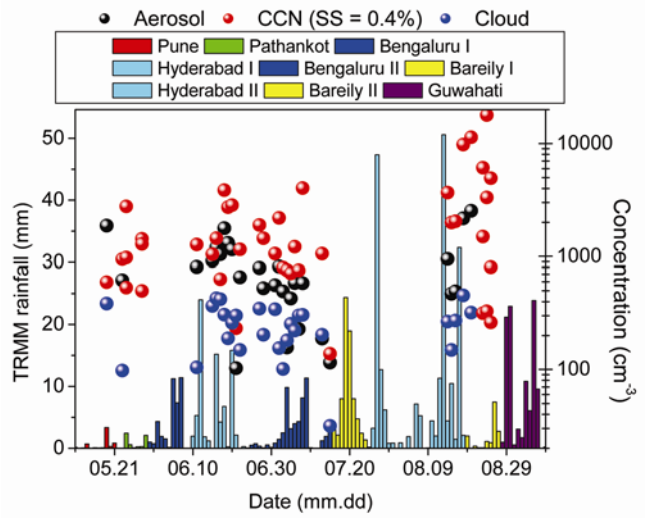

Figure 3. Tropical Rainfall Measuring Mission (TRMM) rainfall (1° × 1° area around CAIPEEX IOP locations (Table 1) as marked in the map). Cloud-averaged droplet number concentration; aerosol number concentration and CCN number concentration from CAIPEEX aircraft observations are presented.

Aerosol and CCN profiling during CAIPEEX phase-I

Aerosol and CCN (concentration) vertical profiles at different locations are shown in Figure 4 *a* and *b*. Aerosol and CCN concentrations along the flight tracks indicated large spatial variability (shown by the error bars). It is of interest to note the strong elevated pollution layer around 1–4 km at Pathankot on 24 May. Highest concentration is observed at elevated layers between 1 and 4 km, and not at the surface. Corresponding CCN observations show a maximum in the boundary layer with a dip at 1.5 km and near-constant values until 5 km. These observations were taken during the prevailing pre-monsoon, dry, supercontinental conditions. The orographic effects in this region (Kashmir Valley) are found to have a crucial role in the elevated aerosol layer that is directly linked to the local circulation patterns adhering to the slopes, which brings valley pollution to elevated layers (more detailed study in this regard is under review; *J. Geophys. Res.*). At elevations above 1 km, long-range transport from the Middle Eastern region with mid-level trajectories showed a subsidence in the Kashmir Valley, as reported by Krishnamurti *et al.*[26].

On 11 June 5-km deep aerosol layer was noticed over Hyderabad with CCN concentration > 1000 cm^{-3} in this thick layer with mid-level flow and with continental air-mass characteristics. On 13 July at Bengaluru, there were very less aerosol and CCN concentrations with active southwesterly monsoon condition. The occasional increase in the aerosol/CCN concentration at specific levels is attributed to the samples from regions adjacent to the clouds. During active monsoon, the boundary layer aerosol concentrations are higher (> 2000 cm^{-3}) over Bareily (24 August), than those over the peninsular region. These high concentrations are noted throughout the lower 4 km layer, with maximum difference in the boundary layer. The boundary layer trajectory shows continental influence pertaining to the lower boundary layer and also to large-scale subsidence. The CCN vertical profile showed

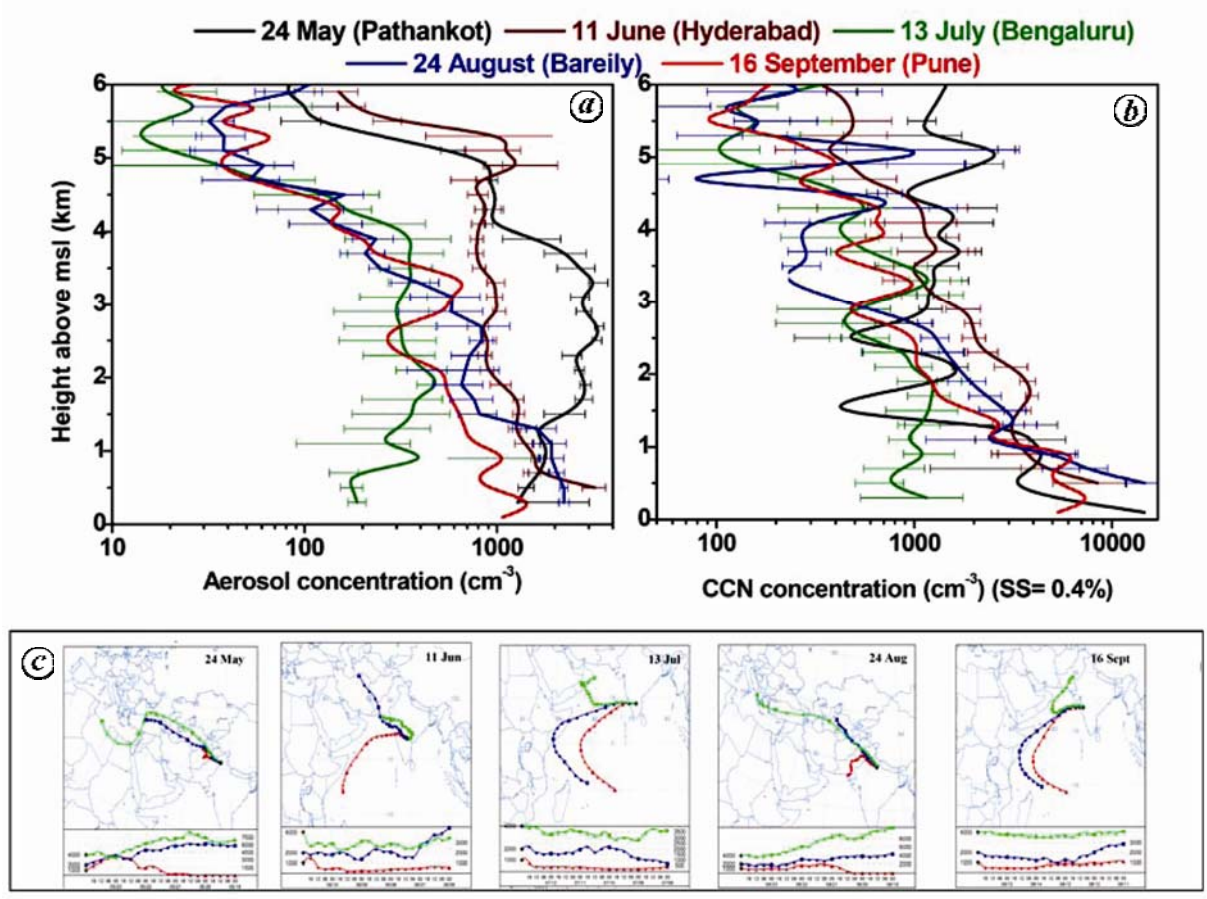

Figure 4. Vertical distribution of aerosol concentrations from (***a***) aerosol and (***b***) CCN concentration at different locations. Each point corresponds to aerosol measurements averaged for every 200 m level and the error bar corresponds to variation within 200 m. All data are cloud-screened. (***c***), The Hysplit backward (5 days) trajectories for the five cases at the respective IOP locations.

good resemblance to the aerosol vertical profiles, indicating the dominance of fine-mode aerosols. Under weak monsoon conditions over Pune region (16 September), there were converging low-level westerlies and northwesterlies in the mid-layer. The low-level NNW light winds prevailing over this region transported pollution from the continental region and the build-up of pollution in the boundary layer.

These results indicate that though there is significant reduction in the aerosol concentration during the active monsoon conditions, replenishment of aerosols in the mid-layer maintains a fairly high ambient concentration of aerosols and CCNs. The minimum average aerosol concentration in the 1–4 km layer is approximately 500 cm^{-3} and that for CCN is 1000 cm^{-3}. High CCN concentration also indicates the presence of fine-mode aerosols. One interesting observation is that there is high (> 1000 cm^{-3}) and uniform concentration of aerosols in a deep layer during the break monsoon conditions, where there is mid-level intrusion of dry air. The existence of Elevated Pollution Layer (EPL) during the different experimental campaigns has been discussed by many researchers[27–30]. In contrast to these studies, during CAIPEEX, we noticed very deep layers with high concentration of aerosols and CCN, sometimes greater than that in the boundary layer or with high concentrations up to 4–5 km. It was noted that aerosol transport to mid-levels was also taking place through vertical mixing from the boundary layers in the presence of a weak inversion layer.

Cloud–aerosol interactions in different monsoon environments

Observations of CDNC and effective radius (r_{eff}) using the CDP probe, boundary layer aerosol concentration (N_a) using the PCASP probe and water vapour mixing ratio (r) using the AIMMS probe are used to illustrate the cloud–aerosol interaction in the monsoon environment. Cloud-averaged effective radius increases with boundary layer water vapour (Figure 5 *a*); cloud droplets grew in size in the moist monsoon environments. Each point in Figure 5 corresponds to a CAIPEEX phase-I observation. In the pre-monsoon dry conditions, the effective radius is well below 10 μm. As indicated in Figure 5 *b*, CDNC is more (300–600 cm^{-3}) in the presence of numerous aerosols

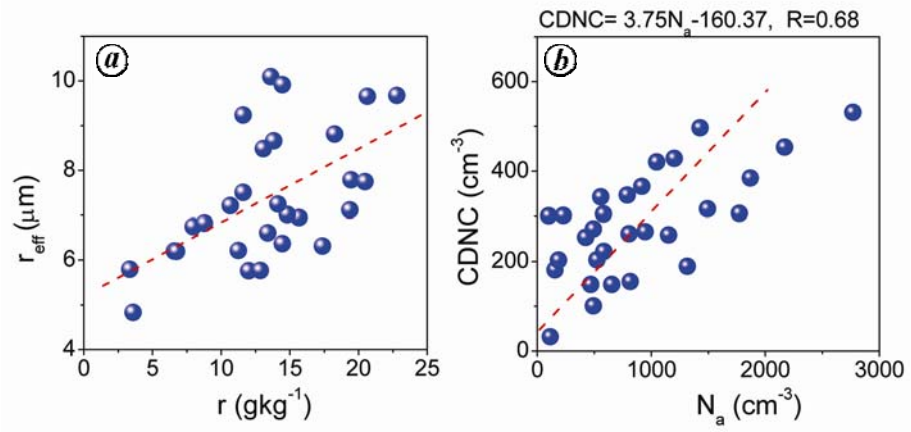

Figure 5. Relation between (***a***) water vapour mixing ratio in the boundary layer and effective radius and (***b***) boundary layer aerosol number concentration and cloud droplet number concentration.

(concentration exceeding 1000 cm^{-3}). Due to the small droplet size (< 10 μm), pre-monsoon droplets are not effective in the collision processes. Growth through diffusion is slow and the droplet spectrum is narrow in these clouds, similar to the reported polluted/smoky cases with decrease in precipitation, characterizing narrow droplet spectra[14,17]. This leads to increase in the height of the collision level, such that raindrop formation is delayed.

A relationship between CDNC and aerosol concentration (CDNC = 3.75 Na–160.37 with a correlation coefficient R = 0.68; Figure 5 *b*) is noted. It has been noticed that moist monsoon conditions characterize incloud nucleation of interstitial aerosol particles and can contribute to the increase in the small droplet number concentrations[31]. This effect was more efficient in the deep clouds during monsoon compared to pre-monsoon conditions.

Black carbon vertical profiling and heating rates

Several studies have reported the presence of BC aerosols in the upper troposphere and lower stratosphere, especially those carried out during the TRACE, INDOEX, ACE-Asia campaigns[32–35]. BC measurements over the Indian region have been undertaken mainly during the ISRO–GBP observational campaigns like the Land Campaign (LC II) conducted in 2004 and the ICARB campaign conducted in 2006 (refs 24, 36–40). Table 5 shows a comparison of results reported by these studies with the present study. Recently, more observations have been made with the help of balloon facility[40]. However, simultaneous observations of aerosol, BC and CCN vertical profiles and cloud microphysical parameters under different environments were lacking until the observations during CAIPEEX[41].

The BC concentrations measured during the aircraft manoeuvring were averaged for every 500 m height to obtain the mean value representing that altitude. All the data points were corrected for temperature and pressure variations. Aircraft measurements of BC mass loadings indicated a decrease with height; however, several intermediate layers containing anomalously high BC loadings were frequently encountered. Figure 6 depicts the vertical profile of BC mass concentration over Bengaluru on 3 June 2009, and over Hyderabad on 11 June 2009. The trajectories on 3 June showed maritime origin in the boundary layer and upper layers. The trajectories showed low-level convergence from the west and mid-level dry-air intrusion from the north and northeast. On 11 June, the low-level westerly convergence was still prevalent. Over Hyderabad, the mean BC mass concentration at the surface was 1665 ng m^{-3}, which decreased to 221 ng m^{-3} at 6 km. Similarly, over Bengaluru, the mean BC concentration at the surface was 1295 ng m^{-3}, which decreased to 70 ng m^{-3} at 6 km. The higher BC concentrations observed in the elevated layers at both the locations can be attributed to convective transport from surface sources. In addition, based on the air-mass trajectories, long-range transport of BC from continental sources is important. Air-mass trajectories showed strong mid-level continental influence for the 11 June case.

The derived BC number density at the surface was used in the optical properties of aerosols and clouds (OPAC) model[42] to derive BC aerosol optical depth, which was incorporated in the Santa Barbara Discrete ordinate Radiative Transfer model (SBDART)[43] to derive shortwave fluxes (0.3–3 μm) at the surface. Also, aircraft-measured vertical profiles of BC, temperature and relative humidity up to 7 km were used. In addition, MODIS-derived columnar water vapour and Ozone Monitoring Instrument (OMI)-derived column ozone values were used. The fluxes were derived for no BC aerosol condition also, and the difference in fluxes with and without BC aerosol condition was calculated for deriving radiative forcing. The rate of change of temperature (dT/dt) in a layer due to radiative heating/cooling is presented in

Table 5. Review of black carbon (BC) measurements in India

Location	Period	BC at the surface (μg)	BC at Maximum altitude (μg)	Reference
Hyderabad (ISRO/LC II)	19–20 February 2004	3.50	0.80 at 2.2 km	36
Kanpur (ISRO/LC II)	4 and 12 January 2004	7.29	1.00 at 1.8 km	37
Kanpur	18 and 19 June 2005	~ 7.50 (FN and AN)	~ 2.5 (FN) at 1.8 km ~ 7.50 (AN) at 1.2 km	38
Bhubaneswar off Bay of Bengal (ISRO/ICARB)	28 March 2006	1.50	1.50 at 3 km	39
Chennai (ISRO/ICARB)	1–8 April 2006	~ 1.80	~ 1.80 at 3 km	40
Hyderabad (ISRO)	March 2010	~ 3	~ 2.5 at ~ 8.5 km	40
Hyderabad (CAIPEEX)	11–21 June 2009	1.668	0.366 at 6.8 km	Present study
Bengaluru (CAIPEEX)	27 and 28 June 2009, 1–3 July 2009	4.849	0.214 at 7 km	Present study

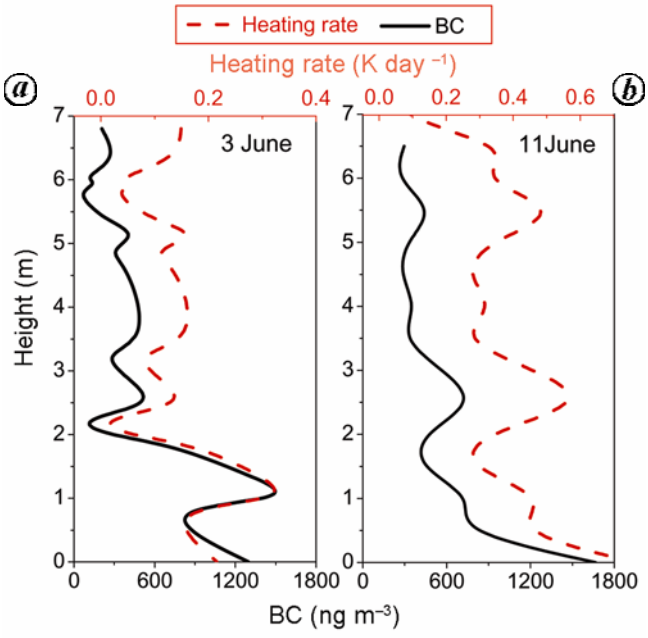

Figure 6. Mean vertical profile of BC mass concentration along with heating rates on 3 June over Bengaluru (***a***) and on 11 June over Hyderabad (***b***).

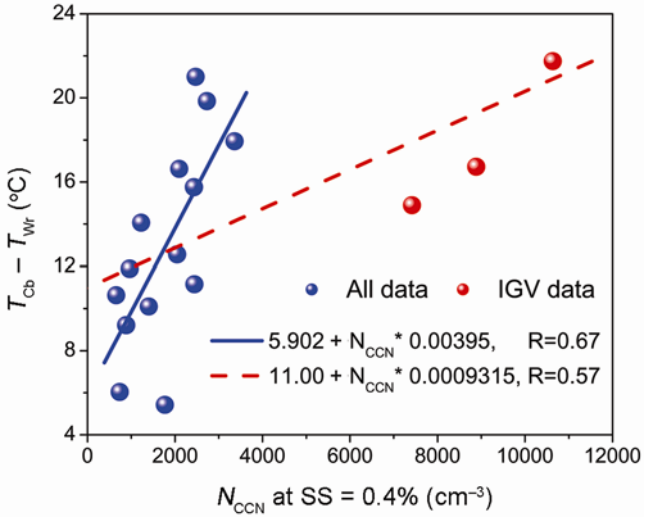

Figure 7. Relationship between CCN concentration (cm^{-3}) at cloud base and difference between cloud base temperature (T_{Cb}) and warm rain onset temperature (T_{Wr}; °C) in growing convective clouds. Straight lines are the least square linear fits to the data and are shown with (a correlation coefficient $R = 0.57$) and without (a correlation coefficient $R = 0.67$) data from Bareilly in the Indian Ganges Valley (IGV).

Figure 6. BC-induced atmospheric heating rates were found to follow the same pattern as those of the vertical BC profiles for that period. The heating rate is higher than 0.2 K day^{-1} and varies to maximum of 0.4 K day^{-1} for elevated layers with high BC mass. For 3 June, the maritime influence dominates in the upper layers. Heating rate is considerably low compared to 11 June. The instantaneous BC aerosol-induced radiative forcing over Hyderabad for 11 June 2009 was –19.5 and 9.5 Wm^{-2} over the surface and top of the atmosphere (TOA) respectively.

Warm rain initiation, role of pollution and critical cloud effective radius

As mentioned earlier, existence of high concentration of aerosols and hence CCN may lead to distribution of the available liquid water content onto a large number of small drops. The data during CAIPEEX phase-I were examined to determine the level at which warm rain initiation takes place as a function of CCN at cloud base. Figure 7 shows that with increase in CCN concentration, the temperature difference between the cloud base (T_{Cb}) and warm rain onset temperature (T_{Wr}) increases. In other words, higher the CCN concentration, higher the temperature difference, i.e. ($T_{Cb} - T_{Wr}$)°C. This means that CCN concentration is an important parameter for the onset of warm rain in the convective clouds. Large CCN concentration reduces the collision–coalescence efficiency of cloud droplets, thus depriving them from forming large droplets, a primary ingredient for the onset of warm rain. However, initiation of warm rain may not only depend on the mean CCN concentration, but also on the distribution of giant CCN at the cloud base and on the presence of updraft velocity. The outliers are the points corresponding to the observations in the highly polluted conditions

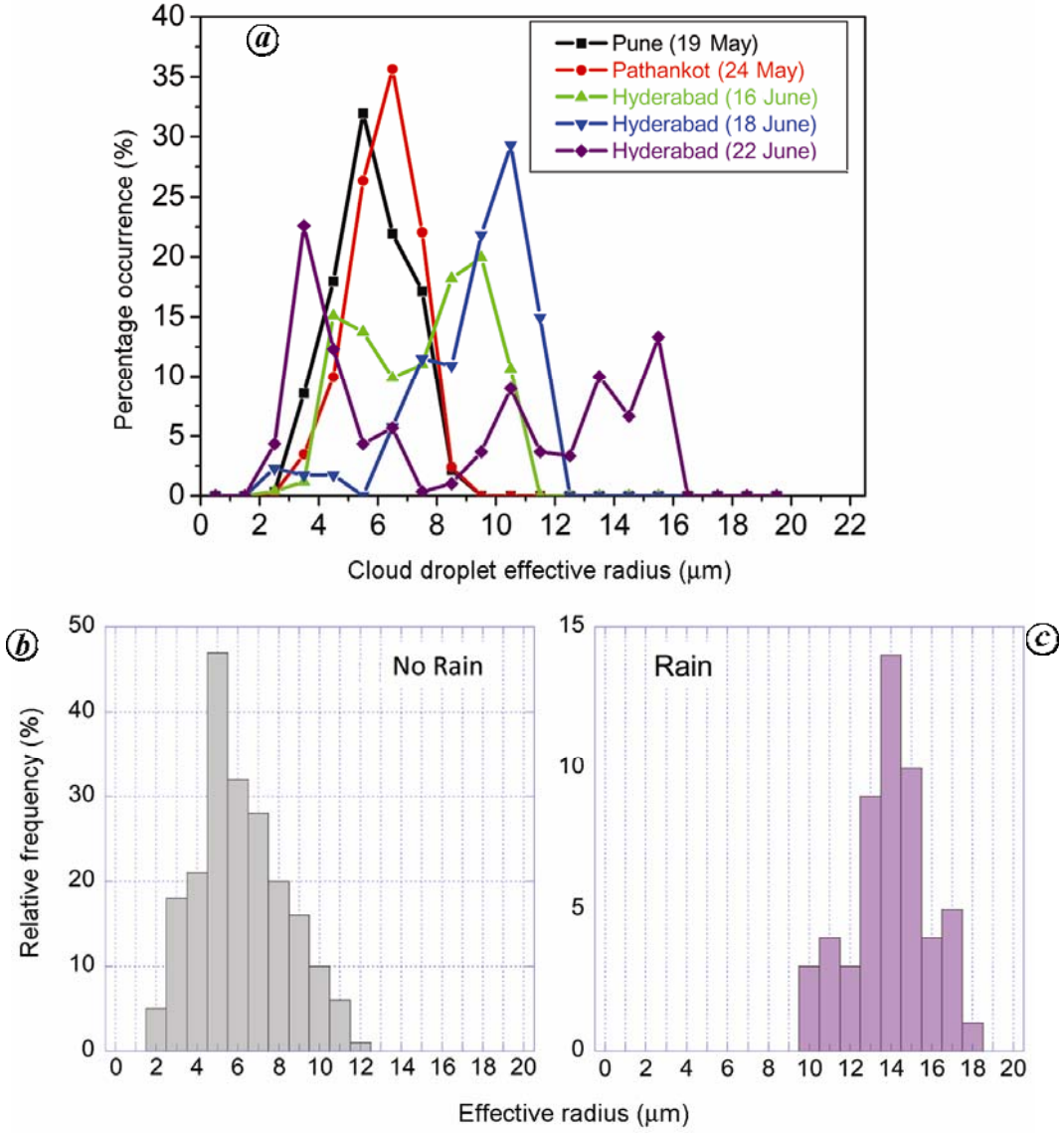

Figure 8. ***a***, Frequency distribution of cloud droplet effective radius over Pune, Pathankot and Hyderabad during the pre-monsosoon and transition to monsoon conditions. Frequency distribution of r_{eff} under no rain (***b***) and rain (***c***) for all cloud observations.

over the Indian Ganges Valley (IGV). Such observations need further detailed study and are outside the scope of this article. Detailed analysis will be carried out on this issue and will be reported elsewhere.

Theoretical calculations[12] and *in situ* observations over other parts of the world[14,44] demonstrated that warm rain formation is initiated if the effective radius (r_{eff}) of cloud droplets exceeds 12 μm, such observations are not available over the continental Asian monsoon environment. As r_{eff} varies with height within the cloud, satellite observations are also inadequate in giving this distribution. An example from the CAIPEEX phase-I observations is given in Figure 8 *a* for the pre-monsoon transition to monsoon conditions to illustrate this aspect. Figure 8 *a* shows frequency distribution of cloud droplet effective radius during pre-monsoon dry conditions over Pune, Pathankot and Hyderabad, and monsoon conditions over Hyderabad. The conditions over Pune on 19 May, Pathankot on 24 May and Hyderabad on 16 June are representative for pre-monsoon conditions. From 18 to 22 June, there was transition to monsoon conditions over Hyderabad. It may be noted that the effective radius is less than 10 μm for Pune and Pathankot, indicating less suitability for seeding. It may also be noted that over Hyderabad, there is a clear transition to higher effective radius exceeding 10 μm. And for monsoon conditions, the bimodal nature of distribution is evident with a peak at smaller drop effective radius and at high effective radius, exceeding the critical effective radius of 14 μm attributed to the incloud nucleation and droplet evapora-

tion[31]. It may also be noted that coexistence of small and large droplets will accelerate collision and coalescence and precipitation formation.

All the observations collected during CAIPEEX phase-I from the CDP when categorized with respect to rain formation indicate that warm rain initiation takes place from cloud droplet size of 10 μm and above. Most frequently, warm rain starts above 12 μm. Drizzle forms from 10 μm onwards and the isolated drops are mostly of the r_{eff} between 8 and 12 μm. At no precipitation condition the cloud droplets were mostly of r_{eff} ranging from 3 to 12 μm. The CDP r_{eff} shows an increasing trend with rain types (from no rain condition to rain through isolated drops and drizzle). To interpret the results in another way, the frequency distribution of r_{eff} for no rain (Figure 8 *b*) and rain (Figure 8 *c*) conditions indicates that the threshold for warm rain at the top of the growing convective cloud is seen beyond 12 μm and is more prominent from 14 μm onwards. However, it should be noted that most of the cloud penetrations targeted non-precipitating clouds and there may be a slight observational bias from the selection of the clouds.

Our results are in general agreement with those of Rosenfeld *et al.*[14] and Freud *et al.*[44]. The value of critical r_{eff} for Indian monsoon clouds is 14 μm (refs 31, 45). This information is useful to assess potential of the clouds for seeding. It is likely that effective radius less than 8 μm may have less amenability to produce rainfall compared to drop effective radius of 10–12 μm. Further studies on the suitability of clouds for seeding based on these observations are underway.

Conclusion

The genesis and scientific basis for conducting CAIPEEX over the Indian monsoon region is described together with state-of-the-art instruments used for a variety of measurements. The objective of this article is to provide the background technical details that would be required for more specific scientific articles to follow. Objectives of both phase-I and phase-II operations are described together with observational strategy for both the phases. However, due to technical constrains, only a few important results from CAIPEEX phase-I are presented in this article. The following are some important results.

- Simultaneous observations of aerosol, CCN and CDNC over the Indian region during monsoon season show very high concentrations (> 1000 cm^{-3}) of CCN at elevated layers.
- Observations of elevated layers with high aerosol concentration over the Gangetic Valley extending up to 6 km and relatively less aerosol concentration in the boundary layer are also documented.
- We also present evidence of strong cloud–aerosol interaction in the moist environments and an increase in the cloud droplet effective radius. CDNC increases with an increase in the aerosol number concentration.
- Our observations also show that pollution increases the warm rain depth and delays its initiation. The critical effective radius for warm rain initiation is found to be between 10 and 12 μm in the polluted clouds, while it is between 12 and 14 μm in cleaner monsoon clouds.

1. Swaminathan, M. S., Abnormal monsoon and economic consequences: the Indian experience. In *Monsoons* (eds Fein, J. S. and Stephens, P. L.), John Wiley, Washington, DC, 1987, pp. 121–133.
2. Xavier, P. K. and Goswami, B. N., Promising alternative to prediction of seasonal mean all India rainfall. *Curr. Sci.*, 2007, **93**, 195–202.
3. Bruintjes, R. T., A review of cloud-seeding experiments to enhance precipitation and some new prospects. *BAMS*, 1999, **80**, 803–820.
4. Todd, C. J. and Howell, W. E., *World Atlas and Catalog of Reported Results of Precipitation Management by Cloud Seeding*, DEC, August 1985, p. 67.
5. Cotton, W. R., Parallels and contrasts between deliberate cloud-seeding and aerosol pollution effects. In *Aerosol Pollution Impact on Precipitation: A Scientific Review* (eds Levin, Z. and Cotton, W. R.), Springer Verlag, 2009, p. 386.
6. Pramanik, S. K. and Koteswaram, P., Heights of tops of low clouds over India. In *Artificial Rain* (ed. Basu, S.), Council of Scientific and Industrial Research, New Delhi, 1955, pp. 104–111.
7. Ramanamurty, B. V. and Biswas, K. R., Weather modification in India. *J. Meteorol. Soc. Jpn.*, 1968, **46**, 160–165.
8. Murty, A. S. R., Mary Selvam, A. and Ramana Murty, Bh. V., Summary of observations indicating dynamic effect of salt seeding in warm cumulus clouds. *J. Appl. Meteorol.*, 1975, **14**, 629–637.
9. Murty, A. S. R., Mary Selvam, A., Paul, S. K., Vijayakumar, R. and Ramana Murty, Bh. V., Electrical and microphysical measurements in warm cumulus clouds before and after seeding. *J. Appl. Meteorol.*, 1976, **16**, 1295–1301.
10. Parasnis, S. S., Selvam, A. M., Murty, A. S. R. and Ramana Murty, Bh. V., Dynamic responses of warm monsoon clouds to salt seeding. *J. Weather Modif.*, 1982, **14**, 35–47.
11. Murty, A. S. R. *et al.*, 11-Year warm cloud-seeding experiments in Maharashtra, India. *J. Weather Modif.*, 2000, **32**, 10–20.
12. Pruppacher, H. R. and Klett, J. D., *Microphysics of Clouds and Precipitation*, Oxford Press, 1997, 2nd edn, p. 914.
13. Feingold, G., Cotton, W. R., Kreidenweis, S. M. and Davis, J. T., The impact of giant cloud condensation nuclei on drizzle formation in stratocumulus: implications for cloud radiative properties. *J. Atmos. Sci.*, 1999, **56**, 4100–4117.
14. Rosenfeld, D. *et al.*, Flood or drought: how aerosols affect precipitation? *Science*, 2008, **321**, 1309–1313.
15. Khain, A., Pokrovsky, A. and Sednev, I., Some effects of cloud–aerosol interaction on cloud microphysics structure and precipitation formation: numerical experiments with a spectral microphysics cloud ensemble model. *Atmos. Res.*, 1999, **52**, 195–220.
16. Rosenfeld, D., Suppression of rain and snow by urban and industrial air pollution. *Science*, 2000, **287**, 1793–1796.
17. Andreae, M. O., Rosenfeld, D., Artaxo, P., Costa, A. A., Frank, G. P., Longo, K. M. and Silva-Dias, M. A. F., Smoking rain clouds over the Amazon. *Science*, 2004, **303**, 1337–1342.
18. Matthews, W. H. (ed.), *Man's Impact on the Global Environment; Assessment and Recommendations for Action*. Report of the Study of Critical Environmental Problems (SCEP), MIT Press, Cambridge, MA, 1970, p. 319.

19. Wilson, C. L., *Study of Man's Impact on Climate: Inadvertent Climate Modification*, MIT Press, Stockholm, 1970, p. 308.
20. Twomey, S., Pollution and the planetary albedo. *Atmos. Environ*., 1974, **33**, 1251–1256.
21. Sikka, D. R., From the International Indian Ocean Experiment (IIOE) to the Arabian Sea Monsoon Experiment (ARMEX) – four decades of major advances in monsoon meteorology. *Mausam*, 2005, **56**, 19–36.
22. Bhat, G. S. and Narasimha, R., Indian summer monsoon experiments. *Curr. Sci.*, 2007, **93**(2), 153–164.
23. Krishnamoorthy, K., Satheesh, S. K., Suresh Babu, S. and Dutt, C. B. S., Integrated Campaign for Aerosols, gases and Radiation Budget (ICARB): an overview. *J. Earth Syst. Sci*., 2008, **117**, 243–262.
24. Babu, S. S., Satheesh, S. K., Krishna Moorthy, K., Dutt, C. B. S., Nair, V. S., Alappattu, D. P. and Kunhikrishnan, P. K., Aircraft measurements of aerosol black carbon from a coastal location in the north-east part of peninsular India during ICARB. *J. Earth Syst. Sci.*, 2008, **117**(S1), 263–271.
25. Baumgardner, D., An analysis and comparison of five water droplet measuring instruments. *J. Climate Appl. Meteorol.*, 1983, **22**, 891–910.
26. Krishnamurti, T. N., Thomas, A., Simon Anu and Vinay Kumar, Desert air incursions, an overlooked aspect, for the dry spells of the Indian Summer Monsoon. *J. Atmos. Sci.*, 2010, **67**, 3423–3441, doi:10.1175/2010JAS3440.1.
27. Ramanathan, V. and Carmichael, G., Global and regional climate changes due to black carbon. *Nature Geosci.*, 2008, doi:10.1038/ngeo156.
28. Ernest Raj, P. *et al.*, Lidar observation of aerosol stratification in the lower troposphere over Pune during pre-monsoon season of 2006. *J. Earth Syst. Sci*., 2008, **117**(S1), 293–302.
29. Satheesh, S. K., Krishna Moorthy, K., Suresh Babu, S., Vinoj, V. and Dutt, C. B. S., Climate implications of large warming by elevated aerosol over India. *Geophys. Res. Lett*., 2008, **35**, L19809, doi:10.1029/2008GL034944.
30. Jai Devi, J., Tripathi, S. N., Gupta Tarun, Singh, B. N., Gopalkrishnan, V. and Dey, Sagnik, Observation-based 3-D view of aerosol radiative properties over Indian Continental Tropical Convergence Zone: implications to regional climate. *Tellus B*, 2011, **63**, 971–989; doi:10.1111/j.1600-0889.2011.00580.x.
31. Prabha, T. V., Khain, A., Maheshkumar, R. S., Pandithurai, G., Kulkarni, J. R., Konwar, M. and Goswami, B. N., Microphysics of pre-monsoon and monsoon clouds as seen from *in situ* measurements during CAIPEEX. *J. Atmos. Sci.*, 2011, **68**, 1882–1901; doi:10.1175/2011JAS3707.1.
32. Blake, D. F. and Kato, K., Latitudinal distribution of black carbon soot in the upper troposphere and lower stratosphere. *J. Geophys. Res*., 1995, **100**, 7195–7202.
33. Pereira, E. B., Setzer, A. B., Gereb, F., Artaxo, P. E., Pereira, M. C. and Monore, G., Airborne measurements of aerosols from burning biomass in Brazil related to Trace A experiment. *J. Geophys. Res*., 1996, **101**, 23983–23992.
34. Mayol-Bracero, O. L. *et al.*, Carbonaceous aerosols over the Indian Ocean during the Indian Ocean Experiment (INDOEX): chemical characterization, optical properties, and probable sources. *J. Geophys. Res. D*, 2002, **107**, 8030; doi:10.1029/2000JD000039.
35. Mader, B. T., Flagan, R. C. and Seinfeld, J. H., Airborne measurements of atmospheric carbonaceous aerosols during ACE-Asia, *J. Geophys. Res. D*, 2002, **107**, 4704; doi:10.1029/2002JD002221.
36. Moorthy, K. K., Suresh Babu, S., Sunilkumar, S. V., Gupta, P. K. and Gera, B. S., Altitude profile of aerosol BC, derived from aircraft measurements over an inland urban location in India. *Geophys. Res. Lett.*, 2004, **31**, 22103.
37. Tripathi, S. N., Dey, S., Satheesh, S. K., Lal, S. and Venkataramani, S., Enhanced layer of black carbon in a north Indian industrial Indian city. *Geophys. Res. Lett.*, 2005, **32**, L12802.
38. Tripathi, S. N., Srivastava, A. K., Dey, S., Satheesh, S. K. and Krishnamoorthy, K., The vertical profile of atmospheric heating rate of black carbon aerosols at Kanpur in northern India. *Atmos. Environ*., 2007, **41**, 6909–6915.
39. Babu, S. S., Krishna Moorthy, K. and Satheesh, S. K., Vertical and horizontal gradients in aerosol black carbon and its mass fraction to composite aerosols over the east coast of Peninsular India from aircraft measurements. *Adv. Meteorol.*, 2010; doi:10.1155/2010/812075.
40. Babu, S. S. *et al*., Free tropospheric black carbon aerosol measurements using high altitude balloon: do BC layers build 'their own homes' up in the atmosphere? *Geophys. Res. Lett*., 2011, **38**, L08803(6); doi:10.1029/2011GL046654.
41. Manoj, M. G., Devara, P. C. S., Safai, P. D. and Goswami, B. N., Absorbing aerosols facilitate transition of Indian monsoon breaks to active spells. *Climate Dyn*., 2010, doi:10.1007/s00382-010-0971-3.
42. Hess, M., Koepke, P. and Schult, I., Optical properties of aerosols and clouds: The software package OPAC. *Bull. Am. Meteorol. Soc*., 1998, **79**, 831–844.
43. Ricchiazzi, P., Yang, S., Gautier, C. and Sowle, D., SBDART: a research and teaching software tool for plane parallel radiative transfer in the Earth's atmosphere. *Bull. Am. Meteorol. Soc.*, 1998, **79**, 2101–2114.
44. Freud, E., Rosenfeld, D., Andreae, M. O., Costa, A. A. and Artaxo, P., Robust relations between CCN and the vertical evolution of cloud drop size distribution in deep convective clouds. *Atmos. Chem. Phys.*, 2008, **8**, 1661–1675.
45. Maheskumar, R. S., Mahen Konwar, Kulkarni, J. R., Goswami, B. N. and Rosenfeld, D., Cloud observations of supercooled rain and its freezing. In Proceedings of Asia Oceania Geosciences Society (AOGS) Conference, Hyderabad, 5–9 July 2010.

ACKNOWLEDGEMENTS. We are grateful to the Ministry of Earth Sciences (MoES), Government of India for funding the experiment. We are also thankful to the National Steering Committee headed by Shri D. R. Sikka, Retd Director, IITM for guidance, encouragement and for his constructive comments on an earlier version of the manuscript. We thank Prof. Daniel Rosenfeld of The Hebrew University of Jerusalem and Dr William L. Woodley, Woodley Weather Consultants, USA and respective team members for guidance and advice during the conduct of the experiment and data quality assessment. We express sincere thanks to India Meteorological Department, National Center for Medium Range Forecasting, National Balloon Facility (TIFR) Hyderabad, Indian Air Force and Indian Navy for the active support provided during the operations.

Received 30 June 2011; revised accepted 21 December 2011